Desalination and Water Treatment
www.deswater.com

doi: 10.5004/dwt.2020.26174

201 (2020) 86–94
October

CFD for the influence of submergence depth of impellers on the flow field and sludge concentration distributions in an oxidation ditch

Wenli Wei*, Ch. Wang, J. Wei, Y. Cai, Y. Chang, B. Lv, Y. Hu

State Key Laboratory of Eco-hydraulics in Northwest Arid Region of China, Xi'an University of Technology, Xi'an, Shaanxi 710048, China, Tel. +86 15596886263; email: wwl_p@126.com (W. Wei), Tel. +86 18591999882; email: 1223942808@qq.com (Ch. Wang), Tel. +86 18629352022; email: Jwei1995@126.com (J. Wei), Tel. +86 15191913820; email: Yxicai@126.com (Y. Cai), Tel. +86 13991987708; email: 564391746@qq.com (Y. Chang), Tel. +86 13822235978; email: lvbin_1@126.com (B. Lv), Tel. +86 13991960738; email: YHu2019_03_18@126.com (Y. Hu)

Received 24 March 2019; Accepted 26 May 2020

ABSTRACT

It is a big problem that the submergence depth of impellers is optimized in an oxidation ditch (OD) to improve mixture flow characteristics and to reduce energy consumption. The mixture model along with the renormalized group κ–ε turbulence model was used to simulate the flow velocity and sludge concentration under different submergence depth ratios of 0.2, 0.4, 0.5, and 0.7 of impellers in an OD, and then the distribution of flow velocity and sludge concentration in the channels were analyzed. The equations for the mixture model was discretized by the finite volume method, and solved by the pressure-implicit with the splitting of Operators algorithm. The results show that, when the submergence depth ratio ranges from 0.4 to 0.5, the velocity and the sludge concentration distributions are more uniform, which can improve the flow field distribution and reduce sludge deposit in an OD; therefore, the range of 0.4–0.5 of submergence depth ratio is optimal and has reference value for the design of ODs.

Keywords: CFD; OD; Submergence depth of impellers; Flow field; Sludge concentration

1. Introduction

OD, known as a "circular aeration tank" or a "continuous loop reactor", originated from Holland in 20th century 50's. The Carrousel OD is one of the mostly used sewage processing technologies, and has advantages of stable operation, good outlet water-quality, and convenient management; therefore, most scholars have carried out numerous experimental and computational studies about it [1–12,14–15]. Lei and Ni [1] proposed a three-dimensional (3D) three-phase fluid model describing water-gas, water-sludge and gas-sludge interactions to simulate the hydrodynamics, oxygen mass transfer, carbon oxidation, nitrification, and denitrification processes in an OD, which can provide detailed phase information on the liquid flow field, gas hold-up distribution, and sludge sedimentation. Li et al. [2] simulated a full-scale OD process for treating sewage so as to optimize it for the minimal cost with acceptable performance in terms of ammonium and phosphorus removal. Xie et al. [3] developed a two-phase (liquid–solid) CFD model for simulating the flow field and sludge settling in a full-scale Carrousel OD, applied the Takács double exponential sedimentation velocity function to simulate the two-phase flow. Yang et al. [4] discussed the influence of the installation position and the submergence depth of surface aerators on dissolved oxygen (DO) concentration distribution. Liu et al. [5] performed experiments by monitoring the amount of sludge, the temperature of sludge, hydraulic retention time, and the DO at the entrance of a Carrousel OD, which found that the optimal DO concentration was mainly affected by the import volume of sewage and its temperature. Xie et

* Corresponding author.

al. [6] carried out a numerical simulation and optimization of an OD to discuss the hydraulic retention time for the anaerobic, anoxic, and aerobic tanks. Fan et al. [7] used CFD methods to simulate the 3D flow fields and hydrodynamic characteristics of an OD driven by inverted umbrella aerators, by which the velocity of liquid phase and solid volume fraction were obtained. The results shows that, the solid vertical velocity is slightly smaller than the liquid velocity, and an increase in reactor velocity leads to an increase in liquid velocity, and makes the solid phase distribution be more uniform in the OD, which are in good agreement with the test data by using particle dynamitic analyzer (PDA). Wu [8] carried out a preliminary study on the problem of sludge distribution, sludge change in an OD with three channels, and pointed out that the larger difference between the sludge concentrations in the three channels was caused by the operation scheme and the time distribution of operation mode, and also pointed out that the sludge concentration difference can be reduced by an increase in the denitrification time. Zeng [9] discussed the sludge age, concentration distribution, sludge discharge, and the effect of the nitrogen and phosphorus removal in triple OD in operation, and put forward an improvement of the design and operation management of triple OD. Sun et al. [10] tested the velocity of OD in a sewage treatment plant, and discussed the effect of the number of impellers and the channel depth on the velocity, which shows that the number of running impellers significantly effects the velocity distribution in space. Sludge deposition phenomenon is easily produced by surface aerators in straight channels; Wu et al. [11] discussed the much non-uniform sludge concentration distribution in OD of a sewage treatment plant, and proposed its solution method. Wei et al. [12] studied the effect of submergence depth of the submerged impellers on the structure of flow fields in an OD by using a two-phase gas–liquid model with 3D Realizable k–ε turbulence model, and obtained an optimal submergence ratio of the submerged depth of impellers to the total water depth, which can help to improve the efficiency of OD sewage treatment system.

Submerged impeller has an important effect on the flow structure in an OD, including the change of its diameter size, rotation speed, and submergence depth. A large part of energy dissipation of OD process comes from the submerged impellers; therefore, finding an optimal submergence depth of impellers with a constant rotation speed and a specified diameter size is very important. In the above literature [1–12], numerous experimental and computational studies have been carried out about the flow fields and sludge concentration distributions in ODs, but few of them are concerned with the influence of submergence depth of impellers. Wei et al. [12] used CFD only to study the effect of submergence depth of submerged impellers on the structure of flow field in an OD, but it does not reflect the sludge concentration distribution. The novelty of this paper is to study the effect of submergence depth of impellers by CFD not only on the flow field but also on the sludge concentration distribution in an oxidation ditch, which has a further step than Wei et al. [12]. This paper used a mixture model with RNG κ–ε model to simulate the flow velocity and sludge concentration under different submergence depth ratios of impellers in an OD with four channels, by which the optimal range of submergence depth of impellers was obtained. In the calculations, the submergence depth of impellers only changes, and other conditions are all fixed.

2. Mixture model

In this study, sewage is considered as a fluid–solid two-phase mixture, fluid (water) is the first phase (main phase); and pollutants are the second phase (solid phase). Therefore, multiphase flow model can be used to simulate the variation of physical parameters of each phase, including the variation of solid volume fraction. Mixture model is a simplified two-phase flow model, which assumes that the coupling between the phases is very strong and uses single-fluid equations to simulate each phase with different velocities. By solving continuity, momentum, and volume fraction equation of second phase, the physical parameters of each phase such as velocity, turbulent kinetic energy, turbulent kinetic energy dissipation rate, and volume fraction of second phase (solid phase) can be obtained. The distribution of solid phase concentration can be further calculated according to the volume fraction of second phase (solid phase). The continuity and momentum equations of mixture phase and the volume fraction equation of a phase can be expressed as [13]:

Continuity equation:

$$\frac{\partial}{\partial t}\left(\rho_m\right)+\nabla\cdot\left(\rho_m\vec{v}_m\right)=\dot{m} \tag{1}$$

Momentum equation:

$$\frac{\partial}{\partial t}\left(\rho_m\vec{v}_m\right)+\nabla\cdot\left(\rho_m\vec{v}_m\vec{v}_m\right)=-\nabla P+\nabla\cdot\left[\mu_m\left(\nabla\vec{v}_m+\nabla^T_{\vec{v}_m}\right)\right]+\rho_m\vec{g}+\vec{F}+\nabla\cdot\left(\sum_{l=1}^{n}\alpha_l\rho_l\vec{v}_{dr,l}\vec{v}_{dr,l}\right) \tag{2}$$

Volume fraction equation of l phase:

$$\frac{\partial}{\partial t}\left(\alpha_l\rho_l\right)+\nabla\cdot\left(\alpha_l\rho_l\vec{v}_m\right)=-\nabla\cdot\left(\alpha_l\rho_l\vec{v}_{dr,l}\right) \tag{3}$$

where ρ_m is the density of mixture phase, $\rho_m=\sum_{i=1}^{n}\alpha_l\rho_l$, where α_l is the volume fraction of l phase, ρ_l is the density of l phase, n is the number of phases; $\vec{v}_m$ is the mass-averaged velocity vector of the mixture phase, and $\vec{v}_m=\frac{\sum_{i=1}^{n}\alpha_l\rho_l\vec{v}_l}{\rho_m}$, where $\vec{v}_i$ is the mass-averaged velocity vector of l phase; $\dot{m}$ is defined as the mass transfer of mass source; P is the pressure; $\vec{F}$ is the volume force vector; $\vec{g}$ is the acceleration vector of gravity; μ_m is viscosity of mixture, and $\vec{v}_{dr,l}$ is the drifting velocity vector of l phase, defined as $\vec{v}_{dr,l}=\vec{v}_l-\vec{v}_m$; n is the number of phases; ∇ is the Hamiltonian operator.

The formula for the computation of the mixture viscosity, μ_m, is expressed as [13]:

$$\mu_m=\rho_m C_\mu\frac{k^2}{\varepsilon} \tag{4}$$

where k and ε are the turbulent kinetic energy and the kinetic energy dissipation rate of the mixture, respectively; C_μ is an empirical constant with a value of 0.085.

3. Turbulence model

Compared to the turbulence models, such as the standard κ–ε model and RNG κ–ε model, the RNG κ–ε model takes into account the effect of turbulent anisotropy, and can better handle large curvature of flow streamline so as to effectively improve the accuracy of computation. Therefore, the RNG κ–ε model is usually adopted for the modeling of turbulence flows in ODs with large curvature of streamlines, the equations of which are expressed as follows [14,15]:

Turbulent kinetic energy k:

$$\frac{\partial(\rho k)}{\partial t}+\frac{\partial(\rho k u_i)}{\partial x_i}=\frac{\partial}{\partial x_j}\left[\left(\mu+\frac{\mu_t}{\sigma_k}\right)\frac{\partial k}{\partial x_j}\right]+G_k-\rho\varepsilon \tag{5}$$

Kinetic energy dissipation rate ε:

$$\frac{\partial(\rho\varepsilon)}{\partial t}+\frac{\partial(\rho\varepsilon u_i)}{\partial x_i}=\frac{\partial}{\partial x_j}\left[\left(\mu+\frac{\mu_t}{\sigma_\varepsilon}\right)\frac{\partial \varepsilon}{\partial x_j}\right]+C_1\frac{\varepsilon}{k}G_k-C_2\rho\frac{\varepsilon^2}{k} \tag{6}$$

where u_i are the time-averaged velocity components in i-direction; and the subscripts i, j = 1, 2, 3; μ is the molecular dynamic viscosity, and μ_t is the turbulence viscosity of mixture, which is also defined as μ_m computed from Eq. (4); G_k is the production term, and $G_k=-\rho\overline{u_i'u_j'}\frac{\partial u_j}{\partial x_i}$; the coefficient $C_1=1.42-\frac{\eta(1-\eta/\eta_0)}{1+\beta\eta^3}$, where $\eta = Sk/\varepsilon$, η_0 = 4.38, β = 0.015, $S=(2S_{i,j}S_{i,j})^{1/2}$, and $S_{i,j}=\frac{1}{2}\left(\frac{\partial u_i}{\partial x_j}+\frac{\partial u_j}{\partial x_i}\right)$; and σ_k, C_2 and σ_ε are empirical constants, and have a value of 0.7179, 1.68, and 0.7179, respectively.

4. Numerical simulation of optimal submergence depth of the impellers

4.1. Calculation region

The test model of OD has four straight channels, labeled as *A*, *B*, *C*, and *D*, each of which has a width of 8.5 m, and a length of 83.5 m. The height of water depth is 4.5 m. The radius of the small bend is R_1 = 8.5 m, and of the big bend is R_2 = 17 m. The impeller consists of eight blades with a length of 1.8 m and a height of 0.7 m. The distance from the center of an impeller to the end of the middle baffle plate (the inner walls) on the horizontal plane is 2.25 m. The calculation region is shown in Fig. 1, the details of which are shown in Fig. 2.

4.2. Grid generation

The grid was generated by the GAMBIT software. The combination of structured and unstructured grids was adopted to generate a high quality calculation grid. The discs and blades were simplified to be infinitely small owing to their thickness being very small compared to the size of the calculation region. The grid with a total number of 265,092 elements was generated, and its independence was performed. Fig. 3a is the 3D grid of the OD, and Fig. 3b shows the 2D plane grid of the OD.

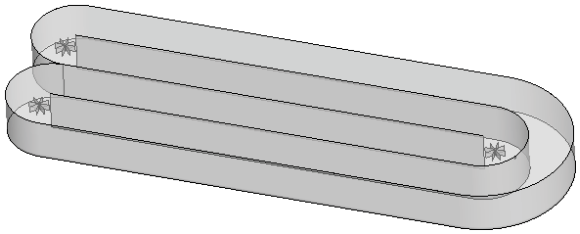

Fig. 1. Computational region.

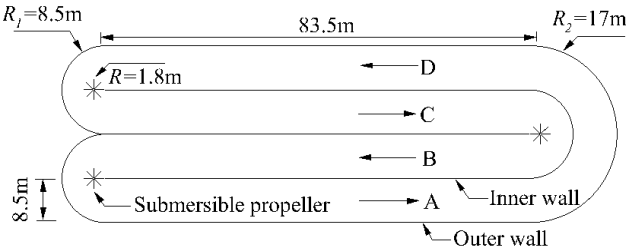

Fig. 2. Details of the computational region.

4.3. Boundary and initial conditions and solution method for the simulation

It has been found that the inlet and outlet conditions have little influence on the flow fields in ODs, so they are ignored in the numerical calculation. Boundary condition at the top surface of the physical model adopted the "rigid-lid" assumption, and at the side walls and the bottom plane was given as a wall-function. The submerged impellers run at a rotation speed of 30 rpm (3.14 rad/s). The motion of the submerged impellers relative to the OD was described by a multiple reference frame model with a sliding mesh method. The initial conditions of the OD are that, the initial water depth was given as 4.5 m, the initial velocity was zero; and the initial sludge concentration was 2,500 mg/L. The calculation time step was 0.005 s, and the total calculation time was 300 s, and the convergence criterion was below 10^{-5}. The control equations were discretized by the finite volume method, and solved by the pressure-implicit with splitting of Operators algorithm.

4.4. Definition of submergence depth ratio of impellers

In order to have an universal significance, the submergence depth of impellers in an OD is described with a dimensionless submergence depth ratio, which is defined as the ratio of the submergence depth, h, of the center of the impellers to the total water height, H, as shown in Fig. 4. Here, we numerically simulated the flow velocity and solid

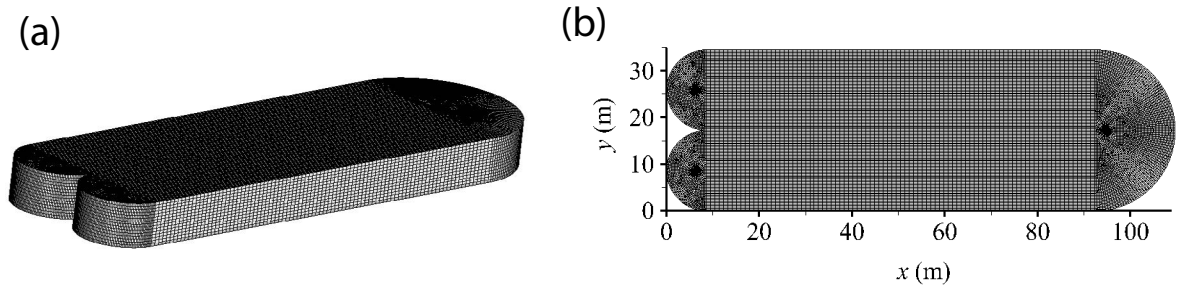

Fig. 3. Grids of the computational domain: (a) 3D grid and (b) 2D plane grid.

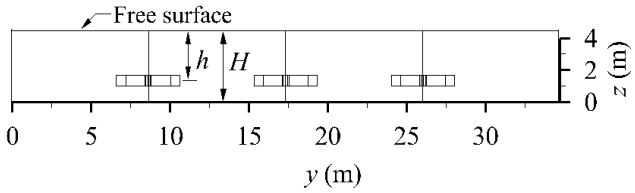

Fig. 4. Submergence depth h of the center point of impellers.

concentration distributions under the four different submergence depth ratios (labeled as h/H), 0.2, 0.4, 0.5, and 0.7, of impellers in the OD.

5. Analysis of the results

5.1. Flow field distributions under different submergence depths of impellers

The combination structure of bend and straight channels of OD easily results in the channel flow distribution be non-uniform, which will retain sludge and affect the performance efficiency of ODs. The submergence depth of impellers has a great influence on the distribution of flow fields in channels. The simulated flow streamlines at different submergence depths, h/H, of impellers, are plotted in Fig. 5.

Figs. 5a–d show the flow field streamline distributions in the lower horizontal plane of z = 1.225 m with different submergence depths, h/H, of impellers; and Figs. 5e–h show the flow field streamline distributions in the upper horizontal plane of z = 3.375 m with different submergence depths, h/H, of impellers. Seen from Figs. 5a–h, the flow field distributions at submergence ratios h/H = 0.4 and 0.5 are more uniform than those of h/H = 0.2 and 0.7. When the submergence ratio of impellers is h/H = 0.2, recirculation zones near the impellers appear at the upper horizontal section of z = 3.375 m in the straight channels, and when the submergence ratio is h/H = 0.7, recirculation zones form at the lower horizontal section of z = 1.225 m, shown in Fig. 5a, which will cause retention of sludge, and is unfavorable for the mixing ability of flow and for the wastewater treatment efficiency of OD. However, both at the upper horizontal section of z = 3.375 m and the lower horizontal section of z = 1.225 m, no matter submergence ratio is h/H = 0.4 or 0.5, recirculation zone does not appear, and the streamline distributions are more uniform in the straight channels of the OD, as shown in Figs. 5c, d, g, and h.

5.2. Concentration field distributions under different submergence depths of impellers

In order to analyze the effect of different submergence depths of impellers on the sludge concentration distribution in the straight channels of OD, the concentration field distributions at the horizontal section of z = 1 m, (a)–(d); and cross-section of x = 50 m, (e)–(h), under different submergence depths of h/H = 0.2, 0.4, 0.5, and 0.7, are plotted in Fig. 6.

Figs. 6a–d show the concentration field distribution at horizontal sections of z = 1 m under different submergence depths of h/H = 0.2, 0.4, 0.5, and 0.7, respectively. With the submergence depth of h/H = 0.7, Fig. 6a shows that, in the small bends, the sludge concentration distributions are non-uniform, and the concentrations near the impellers are relatively great due to the effects of impellers; in addition, at the entrance of the big bends and in the D channel, the sludge concentration is relatively larger. With the submergence depth of h/H = 0.2, Fig. 6b shows that, near the inner wall of the big bend, the sludge concentration increases significantly. With the submergence depth of h/H = 0.4, Fig. 6c shows that, at the outlet of the big bend and in the D channel, sludge concentration is relatively larger. With the submerged depth of h/H = 0.5, Fig. 6d shows that near the outer wall of the big bend and in Channel C, the sludge concentration is relatively larger.

Figs. 6e–h show the concentration field distribution at cross-section of x = 50 m, from which we know that the sludge concentration distributions in Channel A–C are relatively much similar, they were higher at the inside than the outside, and with the submergence ratio of h/H = 0.2, the sludge concentration distribution appears a transverse annular phenomenon. The concentration distributions in Channel D are also different under different submergence depths of h/H = 0.2, 0.4, 0.5, and0.7, respectively. Figs. 6f and g appear obviously that near the water surface the concentration is smaller, but near the bottom is larger, the concentration along the vertical direction appears an obvious stratification phenomenon; while the concentration distribution in Figs. 6e and h appear a transverse annular phenomenon. This phenomenon shows that the submergence depth has a great impact on the distribution of the sludge concentration distribution in the channels; therefore, it is very necessary to find an optimal submergence depth of impellers.

5.3. Distributions of flow velocity and concentration along vertical lines with different submergence depths of impellers

The velocity and sludge concentration distributions along the vertical lines 1–3 in cross-section of x = 50 m in

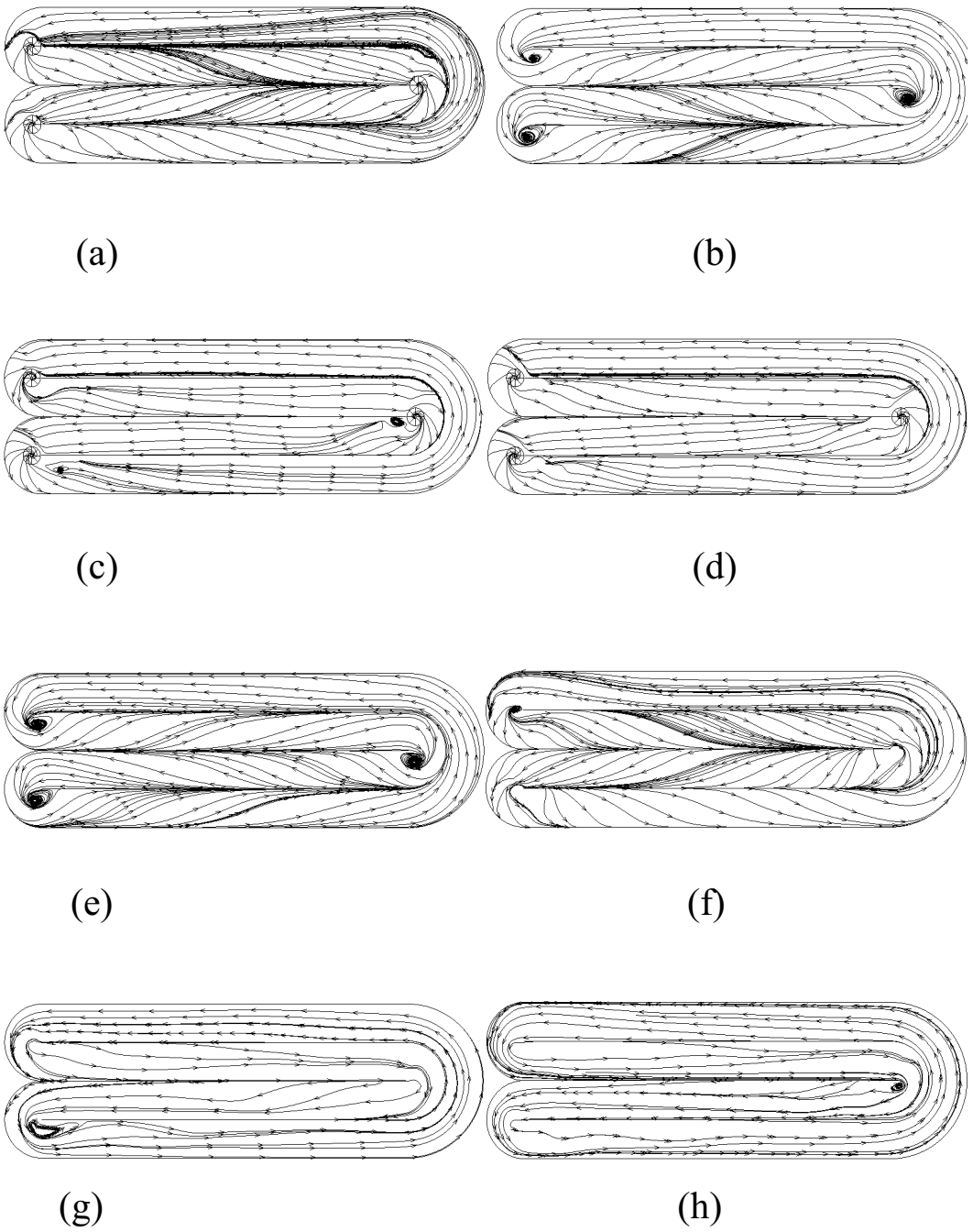

Fig. 5. Computed streamlines in two horizontal planes of z = 1.225 m and 3.375 m, at different submergence depths, h/H of impellers. (a–d) h/H = 0.7, 0.2, 0.4, and 0.5, z = 1.225 m; (e–h) h/H = 0.7, 0.2, 0.4, 0.5, z = 3.375 m.

Fig. 7, were compared between the four submergence depth ratios of h/H = 0.2, 0.4, 0.5, and 0.7 of impellers with the same impeller size and rotation speed, and with the same boundary and initial conditions in the simulations. Fig. 7 shows the three points for the position of the three vertical lines in the section of x = 50 m (in section 2 of Fig. 7).

Figs. 8a–c show the velocity distributions along vertical lines 1–3 under the four submergence depth ratios of h/H = 0.2, 0.4, 0.5, and 0.7 of the impellers. Fig. 8a shows the velocity distribution along the vertical line 1 (at Point 1) in section 2, it can be seen that, with the submergence ratio of 0.7, the total distribution of velocity is the maximum; while with the submergence ratio of 0.2, the velocity is lager at upper part, and smaller at the lower part, and the total distribution of velocity is much uniform, which easily cause sludge deposition at channel bottom; but with the submergence ratios of 0.4 and 0.5, the total distributions of velocity are larger and more uniform, and the more uniform distribution of velocity can prevent the sludge deposition at channel bottom. Fig. 8b shows the velocity distribution along the

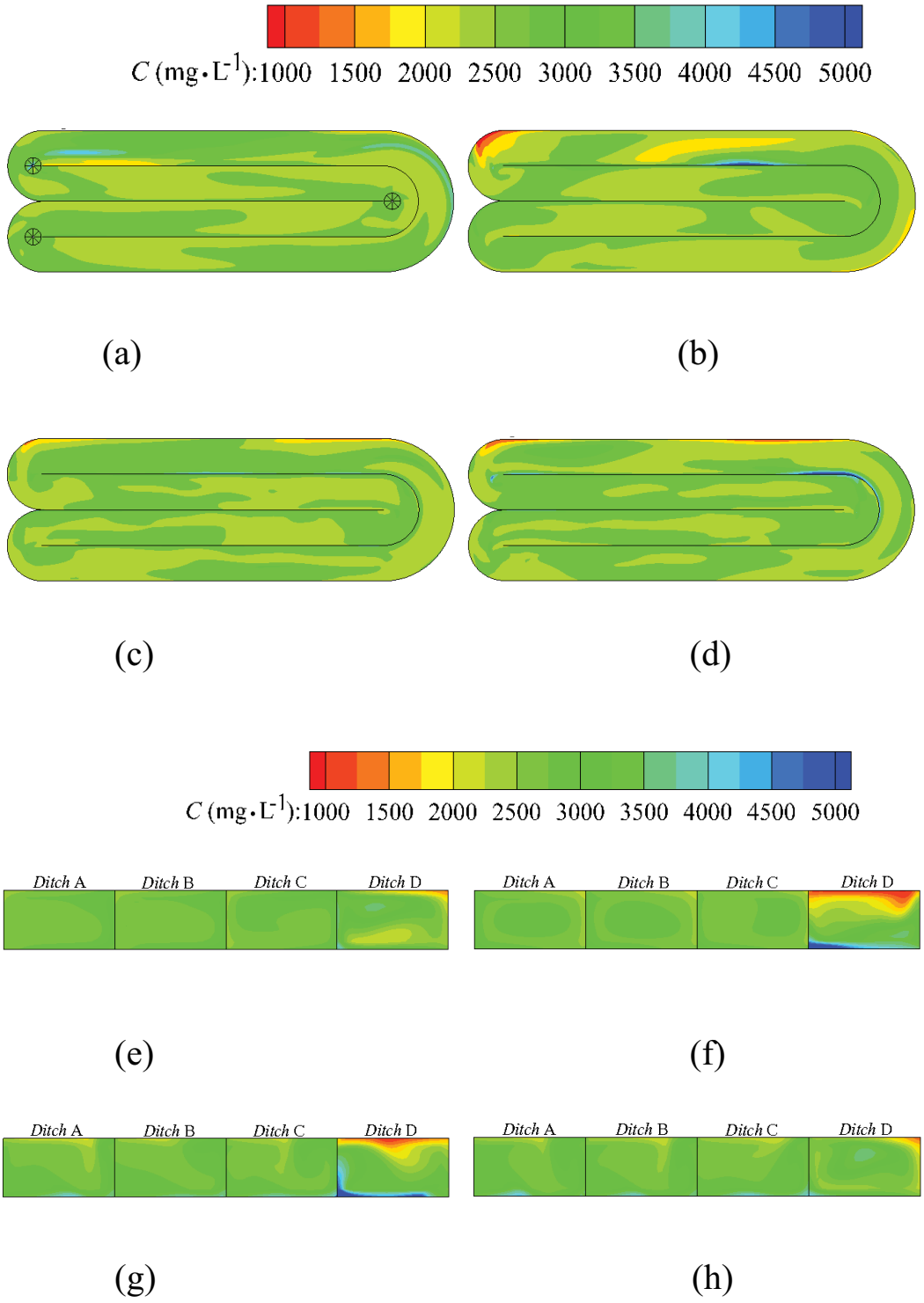

Fig. 6. Computed concentration field distributions at horizontal section of z = 1 m, (a)–(d); and cross section of x = 50 m, (e)–(h), under different submergence depths of h/H = 0.2, 0.4, 0.5, and 0.7, (1 L = 10^{-3} m^3).

vertical line 2 (at Point 2) in section 2, it can be seen that, with the submergence ratios of 0.2 and 0.7, the velocity gradient along the vertical direction is larger, but with the submergence ratios of 0.4 and 0.5 the total distributions of velocity are more uniform. Fig. 8c shows the velocity distribution along the vertical line 3 (at Point 3) in section 2 in the straight channel, it can be seen that, with the submergence ratios of 0.2 and 0.7, the velocity is much larger, but with the submergence ratios of 0.4 and 0.5, the total distributions of velocity are more uniform.

Figs. 8d–f show the sludge concentration distributions along the vertical lines under the four different submergence ratios of h/H = 0.2, 0.4, 0.5, and 0.7 of the impellers, from which it can be seen that the trends of the sludge concentration distributions of the four different conditions are similar, whether it is along the outside, the middle, or the inside vertical line. They all appear smaller at upper part, and greater at lower part.

Whether the sludge concentration distribution is uniform or not has a great effect on improving the sewage treatment efficiency of an OD. As can be seen from Figs. 8d–f, with submergence ratios of h/H = 0.4 and 0.5, the difference between the sludge concentrations along the outside, the middle, or the inside vertical lines is small, and the sludge concentrations are all about 2,500 mg/L. The uniform distribution of concentration is conducive to improve the sewage treatment efficiency of the OD; while with submergence ratios of h/H = 0.7 and 0.2, the difference between the sludge concentrations along the outside, the middle, and the inside vertical lines is great, and the non-uniform distribution of concentration is unfavorable for the removal rate of the OD.

Therefore, no matter from the distribution of the velocity or the sludge concentration, the submergence ratios of h/H = 0.4 and 0.5 is most conducive to improve the processing ability of OD, and to reduce the channel bottom sludge deposition, by which h/H = 0.4–0.5 is the optimal range of submergence ratio of impellers.

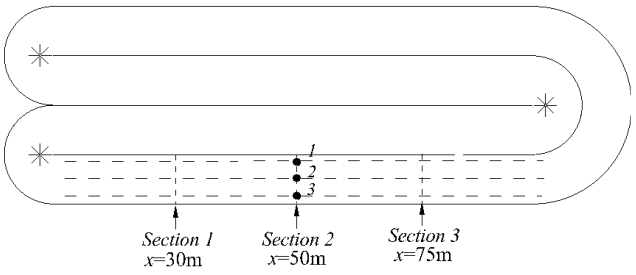

Fig. 7. Location of vertical lines.

6. Discussions and future study plan

Whether the velocity and sludge concentrations of a cross-section are uniform or not is a big problem worthy of attention, because it is directly related to the sludge deposition, DO, and velocity gradient distributions in a ditch. The complicated shape of an OD, action of submerged impellers and surface aerators, and other conditions may result in the flow in straight channels very difficult to achieve a perfect uniformity; therefore, we used CFD method to study the influence of the submergence depth of impellers on the

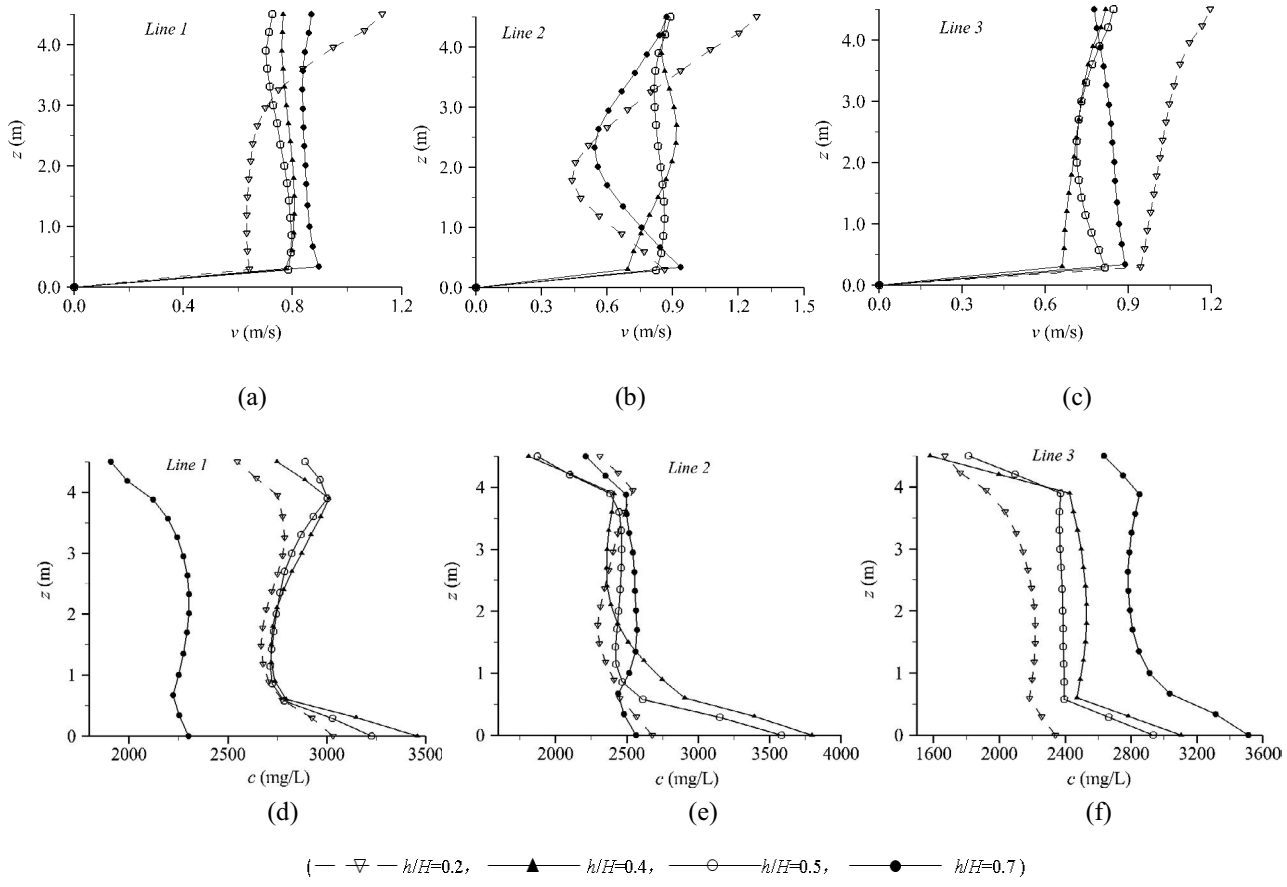

Fig. 8. (a–c) Velocity and (d–f) concentration distributions along vertical lines 1–3 under the four submergence depth ratios of h/H = 0.2, 0.4, 0.5, and 0.7. (1 L = 10^{-3} m^3).

flow field and sludge concentration distributions in an OD. CFD provides a useful tool to study the optimal range of submergence of impellers, by which the optimal range of submergence depth ratio, h/H = 0.4–0.5, was obtained for the OD. According to the actual situation of operation and requirement of sewage treatment, the installation height of impellers cannot be too close to bottom of dich and not too close to the water surface, which is in agreement with the obtained optimal range of submergence depth ratio, h/H = 0.4–0.5. The research result has reference value for reducing the sludge deposit and can improve the efficiency of wastewater treatment for the OD. Of course, the reliability of the research result and the CFD method should be further verified by an experimental method in the future.

An experimental model for the Carrousel OD will be made of organic glass, according to the gravity similarity law (also named Froude number similarity theory) [16]. The different measurement sections in the OD are illustrated with the dashed lines in Figs. 7 and 9. The values of velocity and sludge concentration at some typical points along the vertical lines 1 to 3 in section 2 can be measured, and the measured parameters of the flows in the test model are changed to that of the actual Carrousel OD, and can further be used to compare with the simulation results so as to validate the reliability of the simulation results and the CFD method. After the validating, the CFD method can be used to optimize ODs.

PDA (type 58N50) produced by Dantec cooperation, Denmark, will be applied to measure the flow fields in the OD. It consists of laser, transmitting system, receiver, signal processor, computer, as well as a three-dimensional self-motion shelf, as shown in Fig. 9.

The velocity, diameter, and concentration can be got simultaneously without disturbing the flow field [7]. When two plane polarized laser beams intersect at a measurement point with an angle 2θ, they interfere and create fringes [17]. The two beams have the same intensity, wavelength λ, and polarization. The plane of the fringes is parallel to the bisector of two beams and perpendicular to the flow direction. When the particles in the fluid cross the fringe pattern, they scatter light. The frequency f_D of the scattered light is directly proportional to the flow velocity U of the particle, as given in the equation $|U| = \lambda/(2\sin\theta)\cdot f_D$. Then the optical signal will be converted to an electrical signal by a photo multiplier tube. With the aid of corresponding software, the velocities of liquid and solid could be obtained separately. Details of PDA theory can be found in Fan et al. [7], Bachalo [18], Rashidi et al. [19], and the Dantec PDA manual.

7. Conclusions

The mixture model along with the RNG κ–ε model was used to simulate the flow velocity and sludge concentrations under different submergence depth ratios in an OD, which shows that: within a range of submergence depth ratio of h/H = 0.4–0.5, the uniformity of velocity and sludge concentration are both better. Therefore, the range of 0.4–0.5 of the submergence depth ratio is called the optimal range

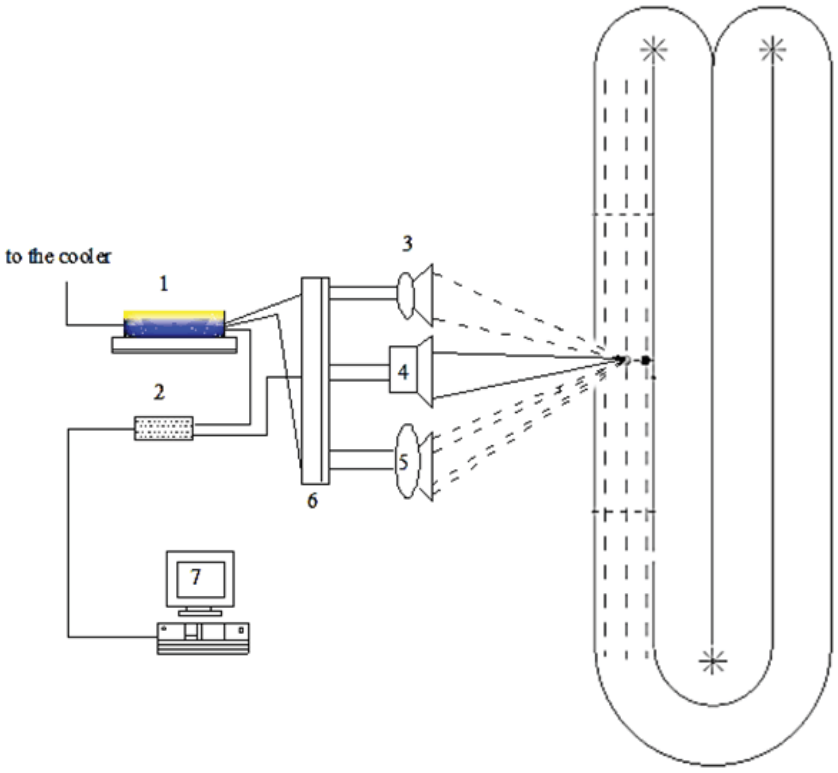

Fig. 9. Sketch of the experimental system and the principle of PDA. (1) Laser, (2) signal processor, (3) one-dimensional fiber-optic probe, (4) receiver, (5) two-dimensional fiber-optic probe, (6) self-motion shelf, and (7) computer.

of submergence depth ratio of impellers. The research result has reference value for reducing the sludge deposit and can improve the efficiency of the wastewater treatment for an OD. Of course, the reliability of the research result will be verified by an experimental method in the future. In addition, CFD can provide a useful tool to study the flow fields and sludge concentration distributions in ODs.

Acknowledgments

Financial support of this study was from the National Natural Science Foundation of China (Grant No. 51578452 and No. 51178391) and the scientific research projects of Shaanxi Province (2020SF-354, 2016GY-180, 15JS063).

Symbols

C	—	Solid concentration, kg/m^3
C_μ	—	Model parameter in Eq. (4) with a value of 0.085
C_1	—	Model parameter in Eq. (6)
C_2	—	Model parameter in Eq. (6) with a value of 1.68
$\vec{F}$	—	Volume force vector, N
$\vec{g}$	—	Acceleration vector of gravity, m/s^2
G_k	—	Production term in Eqs. (5) and (6)
h	—	Submergence depth of impellers, m
H	—	Total water depth, m
k	—	Turbulent kinetic energy, m^2/s^2
$\dot{m}$	—	Mass transfer of mass source, kg
n	—	Number of phases
p	—	Pressure, kg/m×s^2
R_1, R_2	—	Radius of bends, m
S	—	Parameter for computing C_1
$S_{i,j}$	—	Parameter for computing C_1
t	—	Time, s
u_i, u_j	—	Velocity components in i and j directions, respectively, i = 1, 2, 3, m/s; i = 1, 2, 3, m/s
$\vec{v}_{dr,l}$	—	Drifting velocity of l phase, defined as $\vec{v}_{dr,l} = \vec{v}_l - \vec{v}_m$, m/s
$\vec{v}_m$	—	Mass-averaged velocity vector of mixture, m/s
$\vec{v}_l$	—	Mass-average velocity vector of l phase, m/s
x_i, x_j	—	Space coordinates in i and j directions, respectively, i = 1,2,3, m; i = 1,2,3, m

Greek

∇	—	Hamiltonian operator
α_l	—	Volume fraction of l phase
β	—	A constant of 0.015 for computing C_1
ε	—	Kinetic energy dissipation rate, m^2/s^3
η	—	Parameter for computing C_1
η_0	—	A constant of 4.38 for computing C_1
μ_t	—	Turbulent kinematic viscosity, kg/(m × s)
μ_m	—	Viscosity of mixture, kg/(m × s)
ρ_l	—	Density of l phase, kg/m^3
ρ_m	—	Density of mixture, kg/m^3
σ_k	—	Model parameter in Eq. (5) with a value of 0.7197
σ_ε	—	Model parameter in Eq. (6) with a value of 0.7197

Subscripts

dr	—	Drifting velocity
i,j	—	Direction, i = 1, 2, and 3; j = 1, 2, and 3
l	—	Phase
m	—	Mixture
t	—	Turbulence

References

[1] L. Lei, J. Ni, Three-dimensional three-phase model forsimulation of hydrodynamics, oxygen masstransfer, carbon oxidation, nitrification anddenitrification in an oxidation ditch, Water Res., 53 (2014) 200–214.
[2] Z. Li, R. Qi, B. Wang, Z. Zou, G. Wei, M. Yang, Cost-performance analysis of nutrient removal in a full-scale oxidation ditchprocess based on kinetic modeling, J. Environ. Sci., 25 (2013) 26–32.
[3] H. Xie, J. Yang, Y. Hu, H. Zhang, Y. Yang, K. Zhang, X. Zhu, Y. Li, C. Yang, Simulation of flow field and sludge settling in a full-scale oxidation ditch by using a two-phase flow CFD model, Chem. Eng. Sci., 109 (2014) 296–305.
[4] Y. Yang, J. Yang, J. Zuo, Y. Li, S. He, X. Yang, K. Zhang, Study on two operating conditions of a full-scale oxidation ditch for optimization of energy consumption and effluent quality by using CFD model, Water Res., 45 (2011) 3439–3452.
[5] Y. Liu, H. Shi, L. Xia, H. Shi, T. Shen, Z. Wang, G. Wang, Y. Wang, Study of operational conditions of simultaneous nitrification and denitrification in a Carrousel oxidation ditch for domestic wastewater treatment, Bioresour. Technol., 101 (2010) 901–906.
[6] W. Xie, R. Zhang, W.W. Li, B.J. Ni, F. Fang, G.P. Sheng, H.Q. Yu, J. Song, D.Z. Le, X.J. Bi, C.Q. Liu, M. Yang, Simulation and optimization of a full-scale Carrousel oxidation ditch plant for municipal wastewater treatment, Biochem. Eng. J., 56 (2011) 9–16.
[7] L. Fan, N. Xu, Z. Wang, H. Shi, PDA experiments and CFD simulation of a lab-scale oxidation ditch with surface aerators, Chem. Eng. Res. Des., 88 (2010) 23–33.
[8] H. Wu, Three groove type oxidation ditch sewage sludge distribution improved, China Water Wastewater, 17 (2001) 53–55 (in Chinese).
[9] K. Zeng, Three groove type oxidation ditch process wastewater treatment research, Eng. Des. Res., 12 (2013) 32–36 (in Chinese).
[10] X. Sun, H. Zhou, W. Wei, D. Wang, J. Wei, Y. Zhu, Effect of propeller number on flow velocity in oxidation ditch, China Water Wastewater, 29 (2013) 84–86 (in Chinese).
[11] H. Wu, Q. Liu, Q. Li, C. Yang, Problems and solution in operation of oxidation ditch process, Water Wastewater Eng., 28 (2002) 26–28 (in Chinese).
[12] W. Wei, Y. Liu, B. Lv, Numerical simulation of optimal submergence depth of impellers in an oxidation ditch, Desal. Water Treat., 57 (2016) 8228–8235.
[13] W. Wei, Y. Liu, Theory of Multiphase Flow Simulation with Applications in Wastewater Treatment Engineering, Shanxi Science and Technology Press, Xi'an City, China, 2015 (in Chinese).
[14] W. Wei, Z. Zhang, Y. Zheng, Y. Liu, Numerical simulation of additional guiding baffles to improve velocity distribution in an oxidation ditch, Desal. Water Treat., 57 (2016) 24257–24266.
[15] Y. Liu, D. Li, W. Wei, B. Lv, J. Wei, Dimensional analysis and numerical simulation methods for the influence of impellers on the average velocity of flows in an oxidation ditch, Desal. Water Treat., 81 (2017) 26–32.
[16] E. John Finnemore, J.B. Franzini, Fluid Mechanics with Engineering Applications, 10th ed., McGraw-Hill Companies, Inc., New York, NY, 2002.
[17] C.Ü. Yurteri, J.R. Kadambi, E. Arîk, Spray characterization and drop interactions study using particle dynamic analyzer, Laser Anemometry Adv. Appl., 2052 (1993)145–152.
[18] W.D. Bachalo, Method for measuring the size and velocity of spheres by dual beam light scatter interferometry, Appl. Opt., 19 (1980) 363–370.
[19] M. Rashidi, G. Hetsroni, S. Banerjee, Particle–turbulence interaction in a boundary layer, Int. J. Multiphase Flow, 16 (1990) 935–959.